A Switched Systems Approach to Image-Based Localization of Targets That Temporarily Leave the Camera Field of View

Anup Parikh, Teng-Hu Cheng, Ryan Licitra, and Warren E. Dixon

***Abstract*— Image sensors have widespread use in many robotics applications and, in particular, in target tracking. While existing methods assume continuous image feedback, the novelty of this brief stems from the development of dwell time conditions to guarantee convergence of state estimates to an ultimate bound for a class of image-based observers in the presence of intermittent measurements. A Lyapunov analysis for the switched system is performed to develop convergence conditions based on the minimum amount of time the object must be visible and on the maximum amount of time the object may remain outside the camera view. Experimental results are included to verify the theoretical results and elucidate real-world performance.**

***Index Terms*— Computer vision, estimation, range sensing, switched systems, visual tracking.**

I. Introduction

CAMERAS have widespread use in many robotics applications. However, since the imaging process involves a projection of the 3-D scene onto a 2-D imaging plane, resulting in the loss of depth measurements, additional information and processing is required to recover the 3-D coordinates of a target. The depth information can be recovered from multiple views of the target. A typical approach is stereoscopy; however, since all applications exploiting multiple views to recover depth rely on parallax, the operating range for accurate depth recovery from a stereo vision system is limited by the baseline separation between the cameras. In many applications, geometric constraints limit the baseline (e.g., mounting a stereo system on a vehicle), and hence the operating range. Sufficient parallax can be generated by moving a single camera over large distances. This approach is known as structure from motion (SfM) [1].

Online or causal methods typically develop a dynamical system based on the kinematics of the relative position vector between the camera and the target and use dynamical system analysis techniques (e.g., Lyapunov methods) to analyze the evolution of an estimation error signal. In [2]–[8], observers are developed to solve the SfM problem for a stationary target viewed by a moving camera. Similar results have been developed for the reverse case where the camera is stationary while the target is moving, but with known motion [9]–[14]. The results in [15] and [16] are developed for situations where both the target and camera are moving, though with constraints on the unknown target motion relative to the camera.

An underlying assumption in all the aforementioned causal methods is that measurements are continuously available, whereas the development in this brief focuses on causal image-based estimation methods in the presence of intermittent sensing. The estimation error convergence conditions presented in this brief make no assumption on the object motion except that the linear and angular velocities of the target and camera are bounded and, therefore, are applicable to any exponential online method.

In many realistic scenarios, measurements may not be continuously available due to failures in feature tracking due to feature occlusions or features leaving the camera field of view (FOV). In a typical scenario, the estimator is reinitialized with the previous state estimate when the feature is reacquired; however, as shown in [17], switching into a stable system is not sufficient to ensure overall stability of the system, i.e., the estimates may not converge. Moreover, the estimation error dynamics do not converge when the measurements are not available and in fact grow with a bound based on the tangent function as shown in the stability analysis of this brief, and therefore results such as [18] and [19] cannot be used to show overall stability. A contribution of this brief is in the development of the dwell time and reverse dwell time (i.e., minimum and maximum time before switching) requirements for estimator error convergence for uncertain nonlinear dynamics, which exhibit finite escape instabilities.

Robust feature tracking methods have been developed to compensate for scenarios with temporary occlusions. For example, a technique for learning a model of feature motion and using the model to predict feature motion when the object is not visible is developed in [20] and [21]. Similar approaches are developed in [22], where autoregressive models are used for the feature motion and in [23] and [24], where Kalman or particle filters are used for feature motion prediction. In [25]–[27], visual context (i.e., other features around the feature of interest) is used for feature prediction and reacquisition. All of these methods focus on tracking features on the image plane, and must be used with an SfM technique to continuously estimate the 3-D target Euclidean coordinates in the presence of intermittent measurements, but there is no guarantee that the combination will produce a convergent estimate. In contrast, the 3-D coordinates are

Manuscript received July 5, 2017; accepted September 7, 2017. Date of publication October 11, 2017; date of current version October 9, 2018. Manuscript received in final form September 10, 2017. This work was supported in part by NSF under Award 0547448, Award 1161260, and Award 1217908, and in part by a contract with the Air Force Research Laboratory, Munitions Directorate at Eglin AFB. Recommended by Associate Editor S. Tarbouriech. *(Corresponding author: Anup Parikh.)*

A. Parikh, R. Licitra, and W. E. Dixon are with the Department of Mechanical and Aerospace Engineering, University of Florida, Gainesville, FL 32611-6250 USA (e-mail: anuppari@ufl.edu; rlicitra@ufl.edu; wdixon@ufl.edu).

T.-H. Cheng is with the Department of Mechanical Engineering, National Chiao Tung University, Hsinchu 30010, Taiwan (e-mail: tenghu@nctu.edu.tw; tenghu@ufl.edu).

Color versions of one or more of the figures in this paper are available online at http://ieeexplore.ieee.org.

Digital Object Identifier 10.1109/TCST.2017.2753163

estimated in this result, and stability conditions are provided to ensure estimator convergence.

A number of filters have been developed for control and fault detections that are robust to intermittent measurements [28]–[37]. In many of these results [29], [32]–[36], [38]–[43], the measurement loss is modeled with a random variable with a known probability distribution, and only the expected value of the estimation error can be shown to converge. In some results [29], [33], [35], [38], [39], faulty measurements are incorporated in the state estimates, since the measurement loss is assumed to be imperceptible. The results in this brief do not assume the knowledge of the probability distribution used to generate the switching signal, or that such a probability distribution even exists, and faulty measurements are not incorporated into the estimate, since the loss of feature tracking can typically be detected in machine vision applications.

The developments in this brief are made without regard to the cause of measurement unavailability so as to preserve generality. In some cases, measurement unavailability may be arbitrary. In these cases, the stability conditions and performance metrics developed in this brief are useful in determining if enough measurements have been acquired to achieve a desired ultimate bound.

For vehicular systems with motion constraints, guidance and control objectives may be severely restricted if the agent has to move so that the target remains in the FOV [44]–[48]. In such scenarios, the availability of measurements can be controlled. The sufficient dwell time conditions developed in this brief aid in determining when the sensor can be positioned to break the line-of-sight and the maximum time before the target needs to be reacquired.

This brief contrasts with our previous results in [49]. In [49], a predictor is used to continuously estimate the states when the target is not visible; however, this requires knowledge of the target velocities or at least a motion model of the target. In this brief, target velocity information is not required to be known when image measurements are unavailable, leading to different dwell time conditions. This brief also adds value over our preliminary developments in [50]. Compared with [50], the performance of the developed method is examined through experimental results. Moreover, this brief illustrates how a common observer design that only estimates partial states can be extended to full state estimation and therefore can be used while the target is in view.

II. Kinematic Motion Model

The perspective state dynamics $\dot{x} = g(t, x)$, where $g(t, x) : [0, \infty) \times \mathbb{R}^3 \to \mathbb{R}^3$ is a nonlinear function that nonlinearly depends on the partially measurable states can be expressed as

$$\dot{x} = L + Mx + xN^T x \tag{1}$$

where $L,\ N \in \mathbb{R}^3$, $M \in \mathbb{R}^{3\times 3}$ are defined as $L(t) \triangleq [-\omega_2(t),\ \omega_1(t),\ 0]^T$, $N(t) \triangleq [-\omega_2(t),\ \omega_1(t),\ v_{c3}(t) - v_{q3}(t)]^T$

$$M(t) \triangleq \begin{bmatrix} 0 & \omega_3(t) & (v_{q1}(t) - v_{c1}(t)) \\ -\omega_3(t) & 0 & (v_{q2}(t) - v_{c2}(t)) \\ 0 & 0 & 0 \end{bmatrix}$$

$v_q(t) \triangleq [v_{q1}(t)\ v_{q2}(t)\ v_{q3}(t)]^T \in \mathbb{R}^3$ denotes the linear velocities of the target, $v_c(t) \triangleq [v_{c1}(t)\ v_{c2}(t)\ v_{c3}(t)]^T \in \mathbb{R}^3$ denotes the linear velocities of the camera, and $\omega(t) \triangleq [\omega_1(t)\ \omega_2(t)\ \omega_3(t)]^T \in \mathbb{R}^3$ denotes the angular velocity of the camera. As is common in the structure estimation literature, the states of the system are defined as $x = [x_1, x_2, x_3]^T = [(X/Z), (Y/Z), (1/Z)]^T \in \mathbb{R}^3$, where X, Y, and $Z \in \mathbb{R}$ denote the Euclidean coordinates of the target position relative to the camera position, to facilitate the analysis [8]–[10], [13], [51]–[53]. See [54] for the explicit development of (1).

Assumption 1: The state x is bounded, i.e., $x \in \mathcal{X}$, where $\mathcal{X} \subset \mathbb{R}^3$ is a compact set.

Remark 1: Assumptions on state boundedness are required to ensure that the state estimates remain bounded when they converge. This is analogous to assuming boundedness of desired trajectories in tracking control problems. Bounds on the states can be ensured based on the physical constraints on the imaging system during the periods in which the target is in view of the camera. For image formation, the target must remain in front of the camera principle point by at least an arbitrarily small distance, $\epsilon \in \mathbb{R}$. This provides an arbitrarily small lower bound on Z and therefore an arbitrarily large upper bound on x_3. Similarly, a target at an infinite distance ($Z = \infty$) provides a natural lower bound of zero on x_3. Also, the bound on the camera FOV and the bound on Z provide an effective bound on X and Y, therefore bounding x_1 and x_2. During the periods in which the target is not in view, these physical constraints no longer apply. However, Assumption 1 implies that the target does not exhibit finite escape during the unobservable periods. This restricts the relative motion of the target with respect to the camera, i.e., the target cannot move behind the camera, even during the unobservable periods, else the state x_3 will pass through ∞.

Assumption 2: Bounds for the camera and target velocities exist and are known, i.e., $\sup_t |v_{qi}(t)| \le \bar{v}_{qi}$, $\sup_t |v_{ci}(t)| \le \bar{v}_{ci}$, and $\sup_t |\omega_i(t)| \le \bar{\omega}_i \forall i \in \{1, 2, 3\}$, where $\bar{v}_{qi}, \bar{v}_{ci}, \bar{\omega}_i \in \mathbb{R}$ are known nonnegative constants.

Remark 2: Conservative bounds on the target velocities can easily be established. For example, the velocities of observed vehicular systems can readily be upper bounded with some domain knowledge.

To facilitate the subsequent stability analysis, the nonlinear function in (1) can be bounded as

$$\|\dot{x}\| \le \|L\| + \|M\|\|x\|_2 + \|N\|\|x\|_2^2 \tag{2}$$

where $\|\cdot\| \triangleq \sup_t \|\cdot\|_2$, and $\|\cdot\|_2$ refers to the (induced) Euclidean norm of the vector (matrix) $(\cdot)$. From Assumption 2, $\|L\|$, $\|M\|$, and $\|N\|$ are known constants.

Using projective geometry, the image coordinates of the feature point, $p = [u\ v\ 1]^T \in \mathbb{R}^3$, where $u, v \in \mathbb{R}$, are related to the normalized Euclidean coordinates, $m \triangleq [(X/Z)\ (Y/Z)\ 1]^T \in \mathbb{R}^3$, by $p = Am$, where A$\in \mathbb{R}^{3\times 3}$ is the known, invertible camera intrinsic parameter matrix [55]. Since A is invertible, the states x_1 and x_2 are measurable.

III. Structure Estimation Objective

The objective in this brief is to estimate the relative coordinates of the target with respect to the camera despite intermittent measurements. This objective can be accomplished by estimating the state x and then using $[X\ Y\ Z]^T = [(x_1/x_3)\ (x_2/x_3)\ (1/x_3)]$ to recover the relative Euclidean coordinates. To quantify this structure estimation objective, let the state estimate error, $e \in \mathbb{R}^3$, be defined as

$$e = x - \hat{x} \tag{3}$$

where $\hat{x} \in \mathbb{R}^3$ denotes the state estimate provided by an observer. The evolution of e is defined by the family of systems

$$\dot{e} = f_p(t, x, \hat{x}) \tag{4}$$

where $f_p : [0, \infty) \times \mathbb{R}^3 \times \mathbb{R}^3 \rightarrow \mathbb{R}^3$, $p \in \{s, u\}$, s is an index referring to the system in which the target is observable and u is an index referring to the system in which the target is unobservable. When the target is in view, the states x_1 and x_2 are measurable, and the closed-loop error dynamics are given by $f_s = g(t, x) - \dot{\hat{x}}$, where $\dot{\hat{x}}$ is defined by an observer. However, when the target is out of the camera FOV, the state estimates cannot be updated (i.e., $\dot{\hat{x}} = 0$), and the error dynamics are given by

$$f_u = g(t, x). \tag{5}$$

Assumption 3: An observer for the state x has been developed such that, when the states x_1 and x_2 are measurable, the state estimation error is exponentially convergent, i.e., $\|e(t)\| \leq k\|e(t_0)\| \exp[-\lambda_{\text{on}}(t - t_0)]$ for some positive constants $\lambda_{\text{on}}, k \in \mathbb{R}$.

Remark 3: Exponentially convergent observers for the image-based structure estimation are available from results such as [8], [10], [11], [16], [56], and [57]. Any conditions required for implementation and to ensure convergence, e.g., gain conditions, measurement availability assumptions, camera motion requirements, and so on, are also inherited within our approach.

IV. Stability Analysis

In the following development, the switching signal $\sigma : [0, \infty) \rightarrow \{s, u\}$ indicates the active subsystem. Also, let $t_n^{\text{ON}} \in \mathbb{R}$ denote the time of the nth instance at which the target enters the camera FOV and $t_n^{\text{OFF}} \in \mathbb{R}$ denote the time of the nth instance at which the target exits the camera FOV, where $n \in \mathbb{N}$. The dwell time in the nth activation of subsystems s and u is denoted by $\Delta t_n^{\text{ON}} \triangleq t_n^{\text{OFF}} - t_n^{\text{ON}} \in \mathbb{R}$ and $\Delta t_n^{\text{OFF}} \triangleq t_{n+1}^{\text{ON}} - t_n^{\text{OFF}} \in \mathbb{R}$, respectively. Finally, $\Delta t_{\min}^{\text{ON}} \triangleq \inf_{n\in\mathbb{N}}\{\Delta t_n^{\text{ON}}\} \in \mathbb{R}$ and $\Delta t_{\max}^{\text{OFF}} \triangleq \sup_{n\in\mathbb{N}}\{\Delta t_n^{\text{OFF}}\} \in \mathbb{R}$ denote the minimum dwell time in subsystem s and maximum dwell time in subsystem u, respectively, for all n.

Theorem 1: The switched system generated by (4) and switching signal σ is asymptotically regulated to an invariant set, provided that the switching signal and the initial condition satisfy the following sufficient dwell time conditions:

$$\Delta t_{\max}^{\text{OFF}} < \frac{\pi}{2\beta} \tag{6}$$

$$\Delta t_{\min}^{\text{ON}} \geq -\frac{1}{\lambda_s} \ln \frac{1}{\mu^2} \tag{7}$$

$$\frac{1 - \mu^2 \exp\left(-\lambda_s \Delta t_{\min}^{\text{ON}}\right)}{2\mu \exp\left(-\frac{\lambda_s}{2} \Delta t_{\min}^{\text{ON}}\right)} > \tan\left(\beta \Delta t_{\max}^{\text{OFF}}\right) \tag{8}$$

$$c_2\|e(0)\|^2 < \bar{d} \tag{9}$$

where $\beta,\ \lambda_s,\ \mu,\ \bar{d},\ c_2 \in \mathbb{R}$ are known positive bounding constants.

Proof: The existence of an exponentially tracking state observer implies the existence of a Lyapunov function $V_s : [0, \infty) \times \mathbb{R}^3 \rightarrow \mathbb{R}$ that satisfies

$$c_1\|e\|^2 \leq V_s(t, e) \leq c_2\|e\|^2 \tag{10}$$

$$\frac{\partial V_s}{\partial t} + \frac{\partial V_s}{\partial e}(\dot{e}) \leq -c_3\|e\|^2 \tag{11}$$

for some positive scalar constants $c_1,\ c_2,\ c_3 \in \mathbb{R}$, during the periods in which the target is observable [58, Th. 4.14]. From (10) and (11), it is clear that

$$\dot{V}_s \leq -\lambda_s V_s \tag{12}$$

when the target is in view, where $\lambda_s = (c_3/c_2)$.

Consider a Lyapunov-like function $V_u : [0, \infty) \times \mathbb{R}^3 \rightarrow \mathbb{R}$ defined as

$$V_u \triangleq c_5 e^T e \tag{13}$$

where $c_5 \in \mathbb{R}$ is selected so that $c_1 \leq c_5 \leq c_2$. From (10) and (13), it is clear that

$$V_p \leq \frac{c_2}{c_1} V_q, \quad \forall p,\ q \in \{s, u\}, \quad : p \neq q \tag{14}$$

that is for any value of e, the maps V_s and V_u are within a factor $\mu \triangleq (c_2/c_1) \in \mathbb{R}$ of each other. Taking the time derivative of V_u and substituting (2), (4), and (5) yields

$$\dot{V}_u \leq 2c_5(c_6\|e\| + c_7\|e\|^2 + c_8\|e\|^3) \tag{15}$$

where $c_6,\ c_7,\ c_8 \in \mathbb{R}$ denote known positive constants based on the upper bounds on the camera and target velocities and an upper bound on $\|\hat{x}\|$ from Assumption 1. From (13), $\|e\|$ can be upper bounded by $(V_u/c_5)^{1/2}$, resulting in

$$\dot{V}_u \leq \beta\left(V_u^2 + 1\right) \tag{16}$$

where β is a known, bounded, positive constant.

Let the function $W : [0, \infty) \rightarrow \mathbb{R}$ be defined so that $W(t) \triangleq V_{\sigma(t)}(t, e(t))$. From (12) and (16)

$$\dot{W}(t) \leq \begin{cases} -\lambda_s W(t) & t \in \left[t_n^{\text{ON}}, t_n^{\text{OFF}}\right) \\ \beta(W^2(t) + 1) & t \in \left[t_n^{\text{OFF}}, t_{n+1}^{\text{ON}}\right) \end{cases}, \quad \forall n. \tag{17}$$

The second inequality in (17) indicates that W can grow unbounded in finite time when the target is unobservable. However, from the first inequality, W is regulated to zero when the target is observable. This suggests that if the target is observed for a long enough duration and the target is out of the FOV for a short enough duration, the net change in W will be negative over a cycle where observability is lost and regained, and consequently the estimation error will decrease.

Utilizing the Comparison Lemma in [58, Lemma 3.4], (17) can be integrated, yielding

$$W(t) \leq \begin{cases} W_n^s(t) & t \in \left[t_n^{\text{ON}}, t_n^{\text{OFF}}\right) \\ W_n^u(t) & t \in \left[t_n^{\text{OFF}}, t_{n+1}^{\text{ON}}\right) \end{cases}, \quad \forall n \tag{18}$$

where the functions $W_n^s : [t_n^{\mathrm{ON}}, t_n^{\mathrm{OFF}}) \to \mathbb{R}$ and $W_n^u : [t_n^{\mathrm{OFF}}, t_{n+1}^{\mathrm{ON}}) \to \mathbb{R}$ are defined as $W_n^s(t) \triangleq W_n^{\mathrm{ON}} \exp(-\lambda_s (t - t_n^{\mathrm{ON}}))$ and $W_n^u(t) \triangleq \tan(\beta(t - t_n^{\mathrm{OFF}}) + \arctan(W_n^{\mathrm{OFF}}))$, respectively, W_n^{ON} denotes $W(t_n^{\mathrm{ON}})$, and W_n^{OFF} denotes $W(t_n^{\mathrm{OFF}})$. From (14), the discontinuities in W are related by $W(t_n^{\mathrm{OFF}}) \leq \mu W(t_n^{\mathrm{OFF}-})$ and $W(t_{n+1}^{\mathrm{ON}}) \leq \mu W(t_{n+1}^{\mathrm{ON}-})$, where[1] $W(t_n^{\mathrm{OFF}-}) \triangleq \lim_{t \nearrow t_n^{\mathrm{OFF}}} W(t)$ and $W(t_{n+1}^{\mathrm{ON}-}) \triangleq \lim_{t \nearrow t_{n+1}^{\mathrm{ON}}} W(t)$. Therefore, the change in W over a cycle of losing and regaining observability is $W_{n+1}^{\mathrm{ON}} \leq \mu \tan(\beta \Delta t_n^{\mathrm{OFF}} + \arctan(\mu W_n^{\mathrm{ON}} e^{-\lambda_s \Delta t_n^{\mathrm{ON}}})), \forall n$. Considering the worst case scenario of minimum time of observability and maximum unobservability $W_{n+1}^{\mathrm{ON}} \leq \mu \tan(\beta \Delta t_{\max}^{\mathrm{OFF}} + \arctan(\mu W_n^{\mathrm{ON}} e^{-\lambda_s \Delta t_{\min}^{\mathrm{ON}}})), \forall n$, which can be rewritten using a trigonometric identity as $W_{n+1}^{\mathrm{ON}} \leq \mu(A + B W_n^{\mathrm{ON}})/(1 - AB W_n^{\mathrm{ON}})$, where $A = \tan(\beta \Delta t_{\max}^{\mathrm{OFF}})$ and $B = \mu \exp(-\lambda_s \Delta t_{\min}^{\mathrm{ON}})$.

The elements of the sequence $\{W_n^{\mathrm{ON}}\}$ are upper bounded as $W_n^{\mathrm{ON}} \leq z_n, \forall n$, where the sequence $\{z_n\}$ is defined as

$$z_{n+1} = \mu \frac{A + B z_n}{1 - AB z_n} \tag{19}$$

with $z_0 = W_0^{\mathrm{ON}}$. Since the elements of the sequence $\{W_n^{\mathrm{ON}}\}$ are lower bounded by zero due to the definition of W, the squeeze theorem [59, Th. 3.19] can be used to show that $\{W_n^{\mathrm{ON}}\}$ converges to a set upper bounded by $\lim_{n\to\infty} z_n$. The sequence $\{z_n\}$ will converge if it is lower bounded and monotonically decreases. The condition in (6) and the following condition arise from the requirement that z_n remain upper bounded over every iteration from n to $n+1$:

$$AB z_n < 1. \tag{20}$$

For decaying convergence, the sequence is monotonically decreasing for all n if $z_{n+1} \leq z_n$, resulting in the condition

$$AB z_n^2 - (1 - \mu B) z_n + \mu A \leq 0. \tag{21}$$

Since A and B are positive for all positive values of $\Delta t_{\min}^{\mathrm{ON}}$ and $\Delta t_{\max}^{\mathrm{OFF}}$, the inequality in (21) can only be satisfied for various values of z_n if $1 - \mu B \geq 0$, resulting in (7). Note that since $\mu \geq 1$, the left-hand side of (7) is always greater than or equal to zero.

Since the left-hand side of (21) is a convex parabola, the condition $\underline{d} \leq z_n < \bar{d}$ must also be satisfied in addition to the condition in (7), to satisfy the inequality in (21), where $\underline{d}$ and $\bar{d}$ are solutions to the quadratic equation

$$AB z_n^2 - (1 - \mu B) z_n + \mu A = 0 \tag{22}$$

and are given by

$$\underline{d} \triangleq \frac{1 - \mu B - \sqrt{(1 - \mu B)^2 - 4\mu A^2 B}}{2AB}, \tag{23}$$

$$\bar{d} \triangleq \frac{1 - \mu B + \sqrt{(1 - \mu B)^2 - 4\mu A^2 B}}{2AB}. \tag{24}$$

The roots, $\underline{d}$ and $\bar{d}$, are real and distinct if $(1 - \mu B)^2 - 4\mu A^2 B > 0$, which implies (8). If the conditions in (6)–(8) are satisfied and if the initial conditions satisfy (20), the sequence is monotonically decreasing. Since the function $\phi : \mathbb{R} \to \mathbb{R}$, $\phi(z) \triangleq \mu(A + Bz)/(1 - ABz)$, where z is a dummy variable representing the argument of ϕ, is an increasing function on the interval $(-\infty, (1/AB)]$, and $\underline{d}$ and $\bar{d}$ are both upper bounded by $(1/AB)$, $z_n \in [\underline{d}, \bar{d}] \implies \phi(\underline{d}) \leq \phi(z_n) \implies \underline{d} \leq z_{n+1}$. Consequently, if the initial condition z_0 is in the interval $[\underline{d}, \bar{d})$, the sequence is lower bounded and monotonically decreasing and therefore converges. The limit of the sequence is given by $L \triangleq \lim_{n\to\infty} z_n$. Using the definition of the sequence in (19), $\lim_{n\to\infty} z_{n+1} = \mu(A + B\lim_{n\to\infty} z_n)/(1 - AB\lim_{n\to\infty} z_n) \implies L = \mu(A + BL)/(1 - ABL)$, which results in an equation similar to (22) with solutions $L = \underline{d}$ and $L = \bar{d}$. However, since z_n monotonically decreases in the interval $[\underline{d}, \bar{d})$, if $z_0 \in [\underline{d}, \bar{d})$, the sequence $\{z_n\}$ converges to the lesser solution, i.e., $\underline{d}$ and not $\bar{d}$.

A similar procedure can be used to show that z_n monotonically increases outside the interval $[\underline{d}, \bar{d}]$. Again, since ϕ is an increasing function, $z_n \in [0, \underline{d}] \implies \phi(z_n) \leq \phi(\underline{d}) \implies z_{n+1} \leq \underline{d}$. Therefore, if $z_0 \in [0, \underline{d}]$, $\{z_n\}$ monotonically increases and is bounded by $\underline{d}$. Applying the limit as above, it can be shown that $\{z_n\}$ then converges to $\underline{d}$. Thus, if $z_0 \in [0, \bar{d})$ [and therefore automatically satisfies (20)], the elements of the sequence $\{z_n\}$ continue to satisfy (20) and the sequence converges to $\underline{d}$. Consequently, the sequence $\{W_n^{\mathrm{ON}}\}$ converges via the squeeze theorem [59, Th. 3.19] to the interval $0 \leq \lim_{n\to\infty} W_n^{\mathrm{ON}} \leq \underline{d}$. From (18) and the definitions of W_n^s and W_n^u, it is clear that $W(t) \leq W_n^{\mathrm{ON}}, \forall t \in [t_n^{\mathrm{ON}}, t_{n+1}^{\mathrm{ON}}), \forall n$ if conditions (6)–(8) are satisfied. Therefore, $\limsup_{t\to\infty} W(t) \leq \underline{d}$. Using (10), (13), and the definition of W, the estimation error converges to the ultimate bound $\limsup_{t\to\infty} \|e(t)\|^2 \leq (\underline{d}/c_1)$. ■

Remark 4: The observer initial condition, $\hat{x}(0)$, and the state bounds from Assumption 1 can be used to bound the initial error to check the condition in (9) without any additional information. However, satisfying this condition using this initial error bound may require an overly large $\bar{d}$ and therefore overly conservative forward and reverse dwell times (i.e., $\Delta t_{\min}^{\mathrm{ON}}$ and $\Delta t_{\max}^{\mathrm{OFF}}$). Any additional domain knowledge that can be used to restrict $\|e(0)\|$ is helpful in allowing a larger set of dwell times.

Remark 5: The stability conditions in (7) and (8) are functions of the error decay rate, λ_s. The implication of increasing the decay rate of the Lyapunov-like function, i.e., increasing the observer gains, is that the target does not have to remain in the FOV for as long to reach the same ultimate bound. The size of the ultimate bound can also be decreased, either by increasing the dwell time in the observable region or increasing λ_s. However, this is only effective up to a limit. Reexamining (23) and using L'Hôpital's rule, in the limit as $B \to 0$ (i.e., $\lambda_s \to \infty$ or $\Delta t_{\min}^{\mathrm{ON}} \to \infty$), $\underline{d} \to \mu A$, which is equivalent to the growth in W during the period in which the target is out of the camera FOV in the case when the estimation error is initially zero. Similarly, from (24), $\bar{d} \to \infty$ as $B \to 0$, allowing an arbitrarily large initial error.

[1]The notation $\lim_{t \nearrow t*} W(t)$ refers to the one-sided limit of $W(t)$ as t approaches $t*$ from below (i.e., the left-handed limit given in [59, Definition 4.25]).

V. EXPERIMENTS

Experiments were performed to verify the theoretical results. The overall goal of the experiment was to simulate the scenario of tracking the Euclidean position of a cooperative mobile vehicle in a GPS-denied environment via a camera. For example, a common scenario in GPS-denied environments could be one where the object of interest is a cooperative ground vehicle, which is being observed by a high-altitude aerial vehicle with an active GPS signal [60], [61], or when multiple cooperative agents are each observing each other to reduce the overall position uncertainty growth rate [62]–[65]. Specifically, the objective was to demonstrate convergence to an ultimate bound of the relative position estimation errors despite intermittent measurements if a class of image-based observers is used when the mobile vehicle is visible, and a zero-order hold of the position estimate is used when the mobile vehicle is not visible. An IDS UI-1580SE camera with 2-pixel binning enabled and a lens with a 90° FOV was used to capture 1280×960 pixel resolution images at a rate of approximately 15 frames/s. A Clearpath Robotics TurtleBot 2 with a Kobuki base was utilized as a GPS-denied mobile vehicle simulant. An augmented version of the observer in [8] provided range estimates while the mobile robot was visible (details are given in the Appendix). A fiducial marker with a corresponding tracking software library (see [66]) was used to repeatably track the image feature pixel coordinates and the 3-D orientation of the mobile robot while it was in view. Although the library is capable of utilizing marker scale information to reconstruct the fully scaled relative Euclidean position between the camera and the marker, the scale information was not necessary for implementation, and was not used in the experiment. The optic flow signals (i.e., derivatives of the measurable states) required for the observer were approximated via finite difference.

A NaturalPoint, Inc. OptiTrack motion capture system was used to record the ground truth pose of the camera and target at a rate of 360 Hz. The pose provided by the motion capture system was also used to estimate the linear and angular velocities of the camera necessary for the range observer, where the current camera velocity estimates were taken to be the slope of the linear regression of the 20 most recent pose data points. The wheel encoders and rate gyroscope onboard the mobile robot provided estimates of the linear and angular velocity of the robot, expressed in the robot body coordinate system, for input into the range observer. Velocities of both the camera and target are necessary to resolve the well known speed-depth scale ambiguity in vision systems [55, Ch. 5.4.4], and these quantities would be available in a real-world implementation of the scenario considered in this experiment. When the robot was in the camera FOV, the fiducial marker tracking algorithm orientation estimate was used to rotate the linear and angular velocities of the robot into the camera frame, F_C. When the robot was outside the camera FOV, the relative orientation between the camera and robot was estimated via dead-reckoning with the onboard rate gyroscope. For simplicity, the camera was mounted on a stationary tripod, while the TurtleBot was driven via remote control in an unstructured path. The view from the camera can be seen at https://youtu.be/av4OdjOQ4uU.

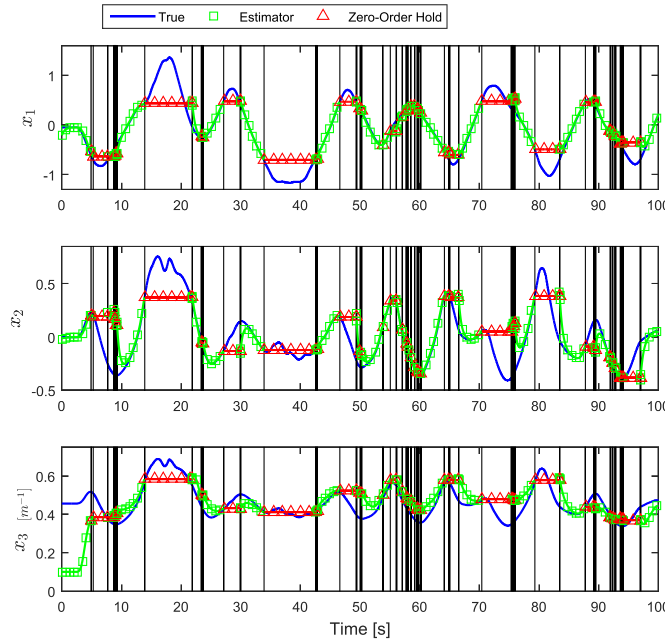

Fig. 1. Evolution of the state estimates during the experiment. Vertical black lines denote switching times. The first vertical line represents the time when the robot is no longer visible, and a zero-order hold is initiated with the last state estimate from the estimator. The second vertical line represents the time when the robot is in view again and the estimator is restarted with the previous state estimate.

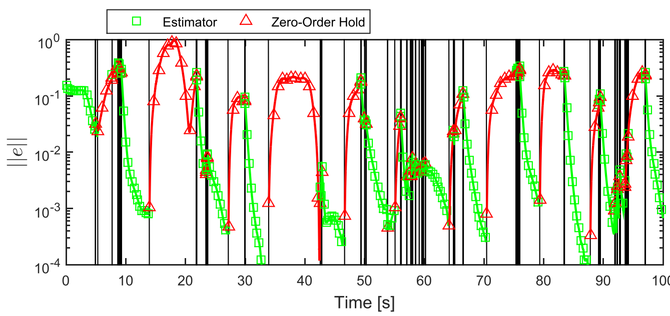

Fig. 2. Evolution of the estimation error. Vertical black lines denote switching times. Note the logarithmic scale.

The results of the experiment are shown in Figs. 1 and 2. From the results, it is clear that the estimation errors remain bounded, as expected based on the analysis in Section IV.

For this experiment, the minimum time the target was in the FOV and the maximum time the target was outside the FOV was $\Delta t_{\min}^{\mathrm{ON}} = 0.95$ s and $\Delta t_{\max}^{\mathrm{OFF}} = 8.7$ s, respectively. The target and camera velocities resulted in a bounding constant $\beta = 4.2$. Based on the minimum dwell time and bounding constants, conditions (6) and (8) dictate that ultimate boundedness of the estimation error is only ensured if $\Delta t_{\max}^{\mathrm{OFF}} < 0.11$s, which would result in an ultimate error of 3.2 m^{-1} rather than approximately 1.0 m^{-1} observed in Fig. 2.

The conservative nature of the Lyapunov analysis was further exemplified by a second set of experiments, performed to examine how the duration of time that measurements are unavailable (i.e., $\Delta t_n^{\mathrm{OFF}}$) affects the ultimate estimation error.

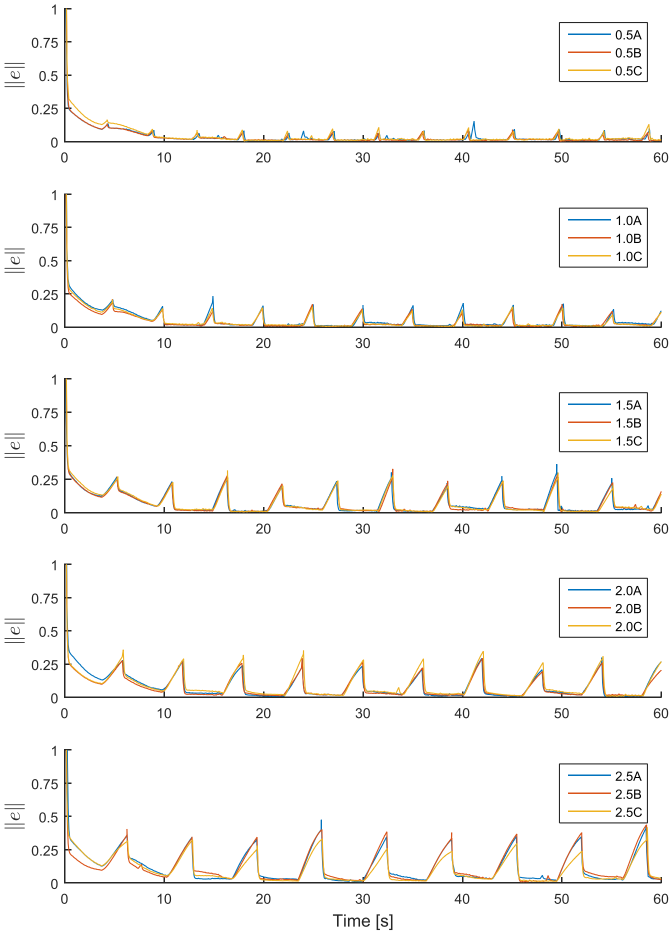

Fig. 3. Evolution of the estimation error for measurement unavailability dwell times of 0.5–2.5 s. Each plot shows three experiments for the listed dwell time.

A number of experiments were performed with $\Delta t_n^{\mathrm{OFF}}$ ranging from 0.5 to 2.5 s, in increments of 0.5 s. During these experiments, Δt_n^{ON} was held constant at 4 s, and the Turtlebot was sent constant forward and angular velocity commands of 0.4 m/s and 0.7 rad/s, respectively, resulting in an approximately circular path. For these target velocities, conditions (6) and (8) dictate that $\Delta t_{\max}^{\mathrm{OFF}} < 1.59$ s. The experiment was performed three times for each set of dwell times. The evolution of the norm of the estimation error for all three runs and across all dwell times is shown in Fig. 3, with the growth of the estimation norm after each period of measurement unavailability shown in Fig. 4 against $\Delta t_n^{\mathrm{OFF}}$. Compared to the bound based on the trigonometric tangent function that was used in the stability analysis, the estimation error in the experiments does not seem to grow unbounded for finite dwell times.

The conservative convergence conditions and ultimate bounds stem from the trigonometric tangent bound of the error growth when the target is not in view. The tangent function exhibits finite escape (i.e., the function approaches infinity for finite inputs), hence additional restrictions are required on $\Delta t_{\max}^{\mathrm{OFF}}$, and $\Delta t_{\min}^{\mathrm{ON}}$ must be comparatively much larger since the estimation error only decays at an exponential rate when the target is in view. The tangent bound itself is a result of the nonlinearities in the system. The bound on the target position is based on a worst case scenario, which can be represented as a sphere that grows with time based on the maximum target velocity bound. When that sphere intersect the imaging plane, the target Z coordinate reaches zero, and therefore the states approach infinity.

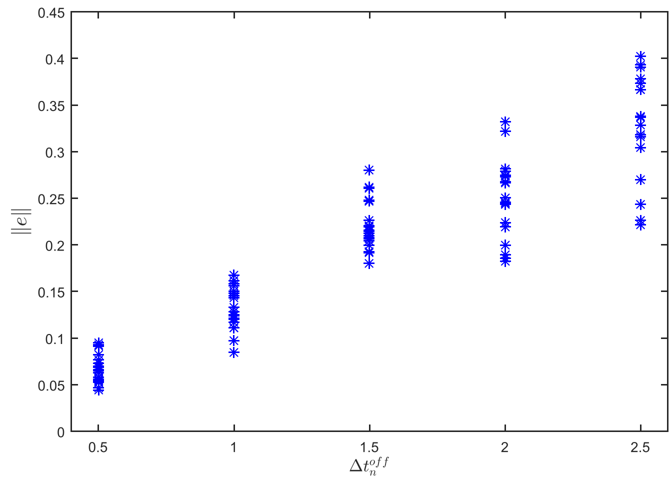

Fig. 4. Growth in the estimation error during each period of measurement unavailability.

The convergence conditions may be slightly relaxed by modifying the stability analysis to consider k cycles of the target entering and leaving view, and requiring that a sequence of W at every kth cycle monotonically decrease. However, this approach would have very limited utility as the condition (6) would still be required due to the finite escape behavior.

VI. Conclusion

This brief focuses on analyzing the stability of a class of image-based range observers in the presence of intermittent measurements. It is shown that in the simple case of implementing a ZOH when measurements are not available, the overall estimation error converges to an ultimate bound, provided a set of dwell time conditions are satisfied. The dwell time conditions were developed by bounding the growth of a Lyapunov-like function during periods in which measurements are not available with the trigonometric tangent function, and analyzing a bounding sequence of the Lyapunov-like functions at the switching instances. Although simplistic, a ZOH is useful in cases where limited target information is available (only bounds on the target velocity is needed, rather than real time measurements of the target velocities, or a motion model of the target). This approach also more accurately reflects the estimator signal when implementing any exponential image-based observers with image measurements at a finite frame rate. Future work will investigate adaptive methods to learn a model of the target motion online, which can be used in conjunction with a predictor to improve estimation performance when the target is not in view, and relax dwell time conditions.

Appendix

In [8], an observer is designed for the unmeasurable state, x_3, whereas it is assumed the estimates for the first two states, x_1 and x_2, are directly measurable. If this design were directly implemented, the state estimates may discontinuously jump whenever the target comes into view, violating the continuity assumption of Theorem 1. By using filtered measurements for the complete state estimate, the continuity assumption can be satisfied. The observer used in the experiments described in Section V is a modified version of the observer in [8] and is defined by the update laws

$$\begin{aligned}\dot{\hat{x}}_1 &= h_1\hat{x}_3 + p_1 + k_1 e_1\\ \dot{\hat{x}}_2 &= h_2\hat{x}_3 + p_2 + k_2 e_2\\ \dot{\hat{x}}_3 &= -b_3\hat{x}_3^2 + (x_1\omega_2 - x_2\omega_1)\hat{x}_3 - k_3\left(h_1^2 + h_2^2\right)\hat{x}_3\\ &\quad + k_3 h_1(\dot{x}_1 - p_1) + k_3 h_2(\dot{x}_2 - p_2) + h_1 e_1 + h_2 e_2\end{aligned}$$

where the error signals, $e \triangleq [e_1\ e_2\ e_3]^T \in \mathbb{R}^3$, are defined as $e \triangleq x - \hat{x}$, the velocity signal is defined as $b \triangleq v_q - v_c \in \mathbb{R}^3$, $k_1, k_2, k_3 \in \mathbb{R}$ are positive constants, and the auxiliary signals $h_1, h_2, p_1, p_2 \in \mathbb{R}$ are defined as in [8]. Using the Lyapunov function candidate $V = (1/2)e_1^2 + (1/2)e_2^2 + (1/2)e_3^2$ it can be shown that $\dot{V} \leq -k_1 e_1^2 - k_2 e_2^2 - k_4 e_3^2$ for some positive constant $k_4 \in \mathbb{R}$, using the same bounding arguments and gain conditions as in [8]. Thus, the augmented observer is exponentially convergent.

ACKNOWLEDGMENT

Any opinions, findings and conclusions or recommendations expressed in this material are those of the author(s) and do not necessarily reflect the views of the sponsoring agency.

REFERENCES

[1] S. Ullman, "The interpretation of structure from motion," *Proc. Roy. Soc. London B, Biol. Sci.*, vol. 203, no. 1153, pp. 405–426, Jan. 1979.

[2] R. Spica, P. R. Giordano, and F. Chaumette, "Active structure from motion: Application to point, sphere, and cylinder," *IEEE Trans. Robot.*, vol. 30, no. 6, pp. 1499–1513, Dec. 2014.

[3] A. Martinelli, "Vision and IMU data fusion: Closed-form solutions for attitude, speed, absolute scale, and bias determination," *IEEE Trans. Robot.*, vol. 28, no. 1, pp. 44–60, Feb. 2012.

[4] D. Braganza, D. M. Dawson, and T. Hughes, "Euclidean position estimation of static features using a moving camera with known velocities," in *Proc. IEEE Conf. Decision Control*, New Orleans, LA, USA, Dec. 2007, pp. 2695–2700.

[5] O. Dahl, Y. Wang, A. F. Lynch, and A. Heyden, "Observer forms for perspective systems," *Automatica*, vol. 46, no. 11, pp. 1829–1834, Nov. 2010.

[6] N. Zarrouati, E. Aldea, and P. Rouchon, "So(3)-invariant asymptotic observers for dense depth field estimation based on visual data and known camera motion," in *Proc. Amer. Control Conf.*, Montreal, QC, Canada, Jun. 2012, pp. 4116–4123.

[7] A. Chiuso, P. Favaro, H. Jin, and S. Soatto, "Structure from motion causally integrated over time," *IEEE Trans. Pattern Anal. Mach. Intell.*, vol. 24, no. 4, pp. 523–535, Apr. 2002.

[8] A. P. Dani, N. R. Fischer, Z. Kan, and W. E. Dixon, "Globally exponentially stable observer for vision-based range estimation," *Mechatronics*, vol. 22, no. 4, pp. 381–389, Jun. 2012.

[9] D. Karagiannis and A. Astolfi, "A new solution to the problem of range identification in perspective vision systems," *IEEE Trans. Autom. Control*, vol. 50, no. 12, pp. 2074–2077, Dec. 2005.

[10] X. Chen and H. Kano, "A new state observer for perspective systems," *IEEE Trans. Autom. Control*, vol. 47, no. 4, pp. 658–663, Apr. 2002.

[11] L. Ma, C. Cao, N. Hovakimyan, C. Woolsey, and W. E. Dixon, "Fast estimation for range identification in the presence of unknown motion parameters," *IMA J. Appl. Math.*, vol. 75, no. 2, pp. 165–189, 2010.

[12] G. Hu, D. Aiken, S. Gupta, and W. E. Dixon, "Lyapunov-based range identification for a paracatadioptric system," *IEEE Trans. Autom. Control*, vol. 53, no. 7, pp. 1775–1781, Aug. 2008.

[13] W. E. Dixon, Y. Fang, D. M. Dawson, and T. J. Flynn, "Range identification for perspective vision systems," *IEEE Trans. Autom. Control*, vol. 48, no. 12, pp. 2232–2238, Dec. 2003.

[14] X. Chen and H. Kano, "State observer for a class of nonlinear systems and its application to machine vision," *IEEE Trans. Autom. Control*, vol. 49, no. 11, pp. 2085–2091, Nov. 2004.

[15] A. P. Dani, Z. Kan, N. R. Fischer, and W. E. Dixon, "Structure and motion estimation of a moving object using a moving camera," in *Proc. Amer. Control Conf.*, Baltimore, MD, USA, 2010, pp. 6962–6967.

[16] A. P. Dani, Z. Kan, N. R. Fischer, and W. E. Dixon, "Structure estimation of a moving object using a moving camera: An unknown input observer approach," in *Proc. IEEE Conf. Decision Control*, Orlando, FL, USA, Dec. 2011, pp. 5005–5012.

[17] D. Liberzon, *Switching in Systems and Control*. Basel, Switzerland: Birkhüuser Verlag, 2003.

[18] G. Zhai, B. Hu, K. Yasuda, and A. N. Michel, "Stability analysis of switched systems with stable and unstable subsystems: An average dwell time approach," *Int. J. Syst. Sci.*, vol. 32, no. 8, pp. 1055–1061, Nov. 2001.

[19] M. A. Müller and D. Liberzon, "Input/output-to-state stability and statenorm estimators for switched nonlinear systems," *Automatica*, vol. 48, no. 9, pp. 2029–2039, 2012.

[20] M. Sznaier and O. Camps, "Motion prediction for continued autonomy," in *Encyclopedia of Complexity and Systems Science*. New York, NY, USA: Springer, 2009, pp. 5702–5718.

[21] M. Sznaier, O. Camps, N. Ozay, T. Ding, G. Tadmor, and D. Brooks, "The role of dynamics in extracting information sparsely encoded in high dimensional data streams," in *Dynamics of Information Systems*, vol. 40. New York, NY, USA: Springer, 2010, pp. 1–27.

[22] F. Xiong, O. I. Camps, and M. Sznaier, "Dynamic context for tracking behind occlusions," in *Proc. Eur. Conf. Comput. Vis.*, Florence, Italy, Oct. 2012, pp. 580–593.

[23] T. Ding, M. Sznaier, and O. Camps, "Receding horizon rank minimization based estimation with applications to visual tracking," in *Proc. IEEE Conf. Decis. Control*, Cancun, Mexico, Dec. 2008, pp. 3446–3451.

[24] M. Ayazoglu, B. Li, C. Dicle, M. Sznaier, and O. I. Camps, "Dynamic subspace-based coordinated multicamera tracking," in *Proc. IEEE Int. Conf. Comput. Vis.*, Barcelona, Spain, Nov. 2011, pp. 2462–2469.

[25] M. Yang, Y. Wu, and G. Hua, "Context-aware visual tracking," *IEEE Trans. Pattern Anal. Mach. Intell.*, vol. 31, no. 7, pp. 1195–1209, Jul. 2009.

[26] H. Grabner, J. Matas, L. van Gool, and P. Cattin, "Tracking the invisible: Learning where the object might be," in *Proc. IEEE Conf. Comput. Vis. Pattern Recognit.*, San Francisco, CA, USA, Jun. 2010, pp. 1285–1292.

[27] L. Cerman, J. Matas, and V. Hlaváč, "Sputnik tracker: Having a companion improves robustness of the tracker," in *Proc. Scandin. Conf. Image Anal.*, Oslo, Norway, Jun. 2009, pp. 291–300.

[28] J. Hu, Z. Wang, H. Gao, and L. K. Stergioulas, "Extended Kalman filtering with stochastic nonlinearities and multiple missing measurements," *Automatica*, vol. 48, no. 9, pp. 2007–2015, Sep. 2012.

[29] Z. Wang, B. Shen, and X. Liu, "H_∞ filtering with randomly occurring sensor saturations and missing measurements," *Automatica*, vol. 48, no. 3, pp. 556–562, Mar. 2012.

[30] S. Dey, A. S. Leong, and J. S. Evans, "Kalman filtering with faded measurements," *Automatica*, vol. 45, no. 10, pp. 2223–2233, Oct. 2009.

[31] B. Sinopoli, L. Schenato, M. Franceschetti, K. Poolla, M. I. Jordan, and S. S. Sastry, "Kalman filtering with intermittent observations," *IEEE Trans. Autom. Control*, vol. 49, no. 9, pp. 1453–1464, Sep. 2004.

[32] K. You, M. Fu, and L. Xie, "Mean square stability for Kalman filtering with Markovian packet losses," *Automatica*, vol. 47, no. 12, pp. 2647–2657, Dec. 2011.

[33] H. Zhang and Y. Shi, "Observer-based H_∞ feedback control for arbitrarily time-varying discrete-time systems with intermittent measurements and input constraints," *J. Dyn. Syst., Meas., Control*, vol. 134, no. 6, Sep. 2012.

[34] B. Shen, Z. Wang, H. Shu, and G. Wei, "On nonlinear H_∞ filtering for discrete-time stochastic systems with missing measurements," *IEEE Trans. Autom. Control*, vol. 53, no. 9, pp. 2170–2180, Oct. 2008.

[35] S. C. Smith and P. Seiler, "Optimal pseudo-steady-state estimators for systems with Markovian intermittent measurements," in *Proc. Amer. Control Conf.*, vol. 4. 2002, pp. 3021–3027.

[36] H. M. Faridani, "Performance of kalman filter with missing measurements," *Automatica*, vol. 22, no. 1, pp. 117–120, 1986.

[37] L. K. Carvalho, J. C. Basilio, and M. V. Moreira, "Robust diagnosis of discrete event systems against intermittent loss of observations," *Automatica*, vol. 48, no. 9, pp. 2068–2078, 2012.

[38] F. O. Hounkpevi and E. E. Yaz, “Robust minimum variance linear state estimators for multiple sensors with different failure rates,” *Automatica*, vol. 43, no. 7, pp. 1274–1280, 2007.

[39] H. Liang and T. Zhou, “Robust state estimation for uncertain discrete-time stochastic systems with missing measurements,” *Automatica*, vol. 47, no. 7, pp. 1520–1524, 2011.

[40] J. Liang, Z. Wang, and X. Liu, “State estimation for coupled uncertain stochastic networks with missing measurements and time-varying delays: The discrete-time case,” *IEEE Trans. Neural Netw.*, vol. 20, no. 5, pp. 781–793, May 2009.

[41] S. Kluge, K. Reif, and M. Brokate, “Stochastic stability of the extended Kalman filter with intermittent observations,” *IEEE Trans. Autom. Control*, vol. 55, no. 2, pp. 514–518, Feb. 2010.

[42] L. Li and Y. Xia, “Stochastic stability of the unscented Kalman filter with intermittent observations,” *Automatica*, vol. 48, no. 5, pp. 978–981, 2012.

[43] S. Deshmukh, B. Natarajan, and A. Pahwa, “Stochastic state estimation for smart grids in the presence of intermittent measurements,” in *Proc. IEEE Latin-Amer. Conf. Commun.*, Nov. 2012, pp. 1–6.

[44] N. R. Gans and S. A. Hutchinson, “A stable vision-based control scheme for nonholonomic vehicles to keep a landmark in the field of view,” in *Proc. IEEE Int. Conf. Robot. Autom.*, Roma, Italy, Apr. 2007, pp. 2196–2201.

[45] S. Bhattacharya, R. Murrieta-Cid, and S. Hutchinson, “Optimal paths for landmark-based navigation by differential-drive vehicles with field-of-view constraints,” *IEEE Trans. Robot.*, vol. 23, no. 1, pp. 47–59, Feb. 2007.

[46] G. López-Nicolás, N. R. Gans, S. Bhattacharya, C. Sagüés, J. J. Guerrero, and S. Hutchinson, “Homography-based control scheme for mobile robots with nonholonomic and field-of-view constraints,” *IEEE Trans. Syst., Man, Cybern. B, Cybern.*, vol. 40, no. 4, pp. 1115–1127, Aug. 2010.

[47] P. Salaris, D. Fontanelli, L. Pallottino, and A. Bicchi, “Shortest paths for a robot with nonholonomic and field-of-view constraints,” *IEEE Trans. Robot.*, vol. 26, no. 2, pp. 269–281, Apr. 2010.

[48] L. R. G. Carrillo, G. R. Flores Colunga, G. Sanahuja, and R. Lozano, “Quad rotorcraft switching control: An application for the task of path following,” *IEEE Trans. Control Syst. Technol.*, vol. 22, no. 4, pp. 1255–1267, Jul. 2014.

[49] A. Parikh, T.-H. Cheng, and W. E. Dixon, “A switched systems approach to vision-based localization of a target with intermittent measurements,” in *Proc. Amer. Control Conf.*, Jul. 2015, pp. 4443–4448.

[50] A. Parikh, T.-H. Cheng, R. Licitra, and W. E. Dixon, “A switched systems approach to image-based localization of targets that temporarily leave the field of view,” in *Proc. IEEE 53rd Annu. Conf. Decision Control*, Dec. 2014, pp. 2185–2190.

[51] J. Civera, A. J. Davison, and J. M. M. Montiel, “Inverse depth parametrization for monocular SLAM,” *IEEE Trans. Robot.*, vol. 24, no. 5, pp. 932–945, Oct. 2008.

[52] B. Ghosh, M. Jankovic, and Y. Wu, “Perspective problems in system theory and its application to machine vision,” *J. Math. Syst. Estim. Control*, vol. 4, no. 1, pp. 3–38, 1994.

[53] R. Abdursul, H. Inaba, and B. K. Ghosh, “Nonlinear observers for perspective time-invariant linear systems,” *Automatica*, vol. 40, no. 3, pp. 481–490, Mar. 2004.

[54] F. Chaumette and S. Hutchinson, “Visual servo control. I. Basic approaches,” *IEEE Robot. Autom. Mag.*, vol. 13, no. 4, pp. 82–90, Dec. 2006.

[55] Y. Ma, S. Soatto, J. Kosecka, and S. Sastry, *An Invitation to 3-D Vision*. New York, NY, USA: Springer, 2004.

[56] A. De Luca, G. Oriolo, and P. R. Giordano, “Feature depth observation for image-based visual servoing: Theory and experiments,” *Int. J. Robot. Res.*, vol. 27, no. 10, pp. 1093–1116, Oct. 2008.

[57] F. Morbidi and D. Prattichizzo, “Range estimation from a moving camera: An immersion and invariance approach,” in *Proc. IEEE Int. Conf. Robot. Autom.*, Kobe, Japan, May 2009, pp. 2810–2815.

[58] H. K. Khalil, *Nonlinear Systems*, 3rd ed. Upper Saddle River, NJ, USA: Prentice-Hall, 2002.

[59] W. Rudin, *Principles of Mathematical Analysis*. New York, NY, USA: McGraw-Hill, 1976.

[60] S. S. Mehta, T. Burks, and W. E. Dixon, “Vision-based localization of a wheeled mobile robot for greenhouse applications: A daisy-chaining approach,” *Comput. Electron. Agricult.*, vol. 63, no. 1, pp. 28–37, 2008.

[61] K. Dupree, N. R. Gans, W. MacKunis, and W. E. Dixon, “Euclidean calculation of feature points of a rotating satellite: A daisy-chaining approach,” *AIAA J. Guid. Control Dyn.*, vol. 31, no. 4, pp. 954–961, 2008.

[62] R. Sharma, S. Quebe, R. W. Beard, and C. N. Taylor, “Bearing-only cooperative localization,” *J. Intell. Robot. Syst.*, vol. 72, nos. 3–4, pp. 429–440, Dec. 2013.

[63] S. I. Roumeliotis and G. A. Bekey, “Distributed multirobot localization,” *IEEE Trans. Robot. Autom.*, vol. 18, no. 5, pp. 781–795, Oct. 2002.

[64] A. I. Mourikis and S. I. Roumeliotis, “Performance analysis of multirobot Cooperative localization,” *IEEE Trans. Robot.*, vol. 22, no. 4, pp. 666–681, Aug. 2006.

[65] X. S. Zhou and S. I. Roumeliotis, “Robot-to-robot relative pose estimation from range measurements,” *IEEE Trans. Robot.*, vol. 24, no. 6, pp. 1379–1393, Dec. 2008.

[66] S. Garrido-Jurado, R. Muñoz-Salinas, F. J. Madrid-Cuevas, and M. J. Marín-Jiménez, “Automatic generation and detection of highly reliable fiducial markers under occlusion,” *Pattern Recognit.*, vol. 47, no. 6, pp. 2280–2292, 2014.